HHS Public Access

Author manuscript

Ultrasound Med Biol. Author manuscript; available in PMC 2015 April 27.

Published in final edited form as:

Ultrasound Med Biol. 2014 September ; 40(9): 2113–2124. doi:10.1016/j.ultrasmedbio.2014.02.027.

PULSED FOCUSED ULTRASOUND TREATMENT OF MUSCLE MITIGATES PARALYSIS-INDUCED BONE LOSS IN THE ADJACENT BONE: A STUDY IN A MOUSE MODEL

Sandra L. Poliachik[*,†], **Tatiana D. Khokhlova**[†,‡], **Yak-Nam Wang**[†], **Julianna C. Simon**[†], and **Michael R. Bailey**[†]

[*]Department of Radiology, Seattle Children's Hospital, Seattle, Washington, USA

[†]Center for Industrial and Medical Ultrasound, Applied Physics Laboratory, University of Washington, Seattle, Washington, USA

[‡]Division of Gastroenterology, Department of Medicine, University of Washington, Seattle, Washington, USA

Abstract

Bone loss can result from bed rest, space flight, spinal cord injury or age-related hormonal changes. Current bone loss mitigation techniques include pharmaceutical interventions, exercise, pulsed ultrasound targeted to bone and whole body vibration. In this study, we attempted to mitigate paralysis-induced bone loss by applying focused ultrasound to the midbelly of a paralyzed muscle. We employed a mouse model of disuse that uses onabotulinumtoxinA-induced paralysis, which causes rapid bone loss in 5 d. A focused 2 MHz transducer applied pulsed exposures with pulse repetition frequency mimicking that of motor neuron firing during walking (80 Hz), standing (20 Hz), or the standard pulsed ultrasound frequency used in fracture healing (1 kHz). Exposures were applied daily to calf muscle for 4 consecutive d. Trabecular bone changes were characterized using micro-computed tomography. Our results indicated that application of certain focused pulsed ultrasound parameters was able to mitigate some of the paralysis-induced bone loss.

Keywords

Pulsed focused ultrasound; Paralysis; Mitigation of trabecular bone loss; Mouse model of disuse; Musculoskeletal; Micro-computed tomography

INTRODUCTION

Bone loss is a common sequela of inactivity and physiologic changes caused by trauma, spinal cord injury, long-term exposure to microgravity and age-related hormonal changes (Jiang et al. 2006; Khosla et al. 2011; Schneider et al. 1995; Sievanen 2010; Williams et al.

Address correspondence to: Sandra L. Poliachik, 4800 Sand Point Way, M/S MA.7.220, Seattle, WA 98105, USA. sandra.poliachik@seattlechildrens.org.

2009; Wronski et al. 1985). Current countermeasures for treating bone loss include several varieties of exercise, pharmacologic treatments and whole body vibration (WBV). A combination of impact loading and resistance exercise has been shown to at least help maintain bone mass in the elderly; however, an optimal exercise regimen has yet to be determined for this population (Bolam et al. 2013). To date, the predominant strategy in the treatment of postmenopausal bone loss has been the use of hormone replacement therapy, which might be limited in the future by adverse side effects and long-term safety concerns (Body 2011; Cusano and Bilezikian 2012; Lacey et al. 2002; Marjoribanks et al. 2012). Bisphosphonate use is currently being tested in conjunction with exercise in a space flight trial (Leblanc et al. 2013). In addition, a WBV method has been tested for training astronauts to prepare for microgravity-induced bone loss, and has been reported to have a positive effect on bone mineral density (Belavy et al. 2011). There is yet to be a consensus, however, as to whether WBV is effective in elderly patients (Liu et al. 2011), and it may not be applicable to patients with immobility-induced bone loss.

In recent years, another therapeutic modality influencing bone conditions has been gaining momentum: pulsed acoustic energy targeting the bone. In particular, acoustic treatment of bone non-unions has been found to be effective in a number of both animal and human studies (Azuma et al. 2001; Elster et al. 2010; Leung et al. 2004b; Rawool et al. 2003; Zelle et al. 2010). Low-intensity pulsed ultrasound (LIPUS) is applied locally to the bone and uses a moderate acoustic intensity from a planar transducer at pulsed frequencies of around 1 kHz to aid in healing of fractures and non-unions. Although LIPUS has been found to reduce healing time in these situations (by up to 38%), the mechanism of action has yet to be fully elucidated (Della Rocca 2009). In addition, extracorporeal shock wave therapy (ESWT) has been used to stimulate healing in fractures with delayed unions or non-unions. ESWT devices deliver high-amplitude, focused shock waves (up to 50 MPa peak positive and 15 MPa peak negative pressures) at a very low pulse repetition frequency (1–4 Hz). These two techniques, ESWT and LIPUS, are strikingly different, yet are reported to provide a similar desired effect of nonunion fracture healing.

Ultrasound has also been used in animal models in an attempt to mitigate bone loss induced by spinal cord injury, ovariectomy and neurectomy, yet the results remain controversial (Carvalho and Cliquet Junior 2004; Cook et al. 2001; Ferreri et al. 2011; Gollwitzer et al. 2013; van der Jagt et al. 2013; Warden et al. 2001a; Yang et al. 2005). In particular, Ferreri et al. (2011) applied LIPUS to the L4 and L5 vertebrae in ovariectomized rats for 20 min daily, 5 d a wk, for 4 wk, and observed partial mitigation of trabecular bone loss compared with the control group. The hypothesized mechanisms for this effect include ultrasound-induced microstreaming caused by local pressure gradients within the bone microstructure, or the generation of an electric field caused by mechanical movement of ionic fluids within the bone. Another author observed similar effects using low-amplitude, unfocused shock waves (van der Jagt et al. 2013), and the hypothesized mechanism was acoustic cavitation. However, the majority of evidence suggests that neither treatment of the intact bone by shock waves nor treatment of the bone by LIPUS is efficient in mitigating bone loss (Carvalho and Cliquet Junior 2004; Warden et al. 2001a; Yang et al. 2005).

The goal of the present study was to evaluate whether bone loss could be mitigated indirectly by targeting the pulsed ultrasound treatment to the muscle adjacent to the bone of interest and potentially stimulating the musculoskeletal environment. To model appendicular bone loss, we employed a mouse model of disuse using onabotulinumtoxinA (Obtx) to induce paralysis of the calf muscle, which results in rapid degradation of trabecular bone in the proximal tibia (Poliachik et al. 2010; Warner et al. 2006) This model has been found to reduce, but not remove, ground reaction forces in the affected limb (Manske et al. 2011).The resulting maximum trabecular bone loss in this model occurs approximately 12 d after Obtx injection; an average of 77% trabecular bone volume was lost in C57B6 mice. Pulsed focused ultrasound (pFUS) mimicking physiologic muscle contraction rates or LIPUS frequency for fracture healing (1 kHz) (Azuma et al. 2001; Leung et al. 2004b) was applied to the calf muscle after paralysis in an attempt to mitigate the associated bone loss. The effect of the intervention on the structure of the trabecular bone in the proximal tibia metaphysis was evaluated with micro-computed tomography (mi-croCT), and the potential damage to the muscle tissue was evaluated via histology.

METHODS

Experiment design

All studies were approved by the University of Washington Institutional Animal Care and Use Committee. Mice were group housed with access to food and water *ad libitum*, with free ambulation. Seven groups of female 16 wk-old C57B6 mice (n = 8 per group) were injected with Obtx (2 U/100 g weight, 20 μL), and one group was injected with saline (20 μL, n = 8), in the midbelly of the right calf on day 0. A group of animals was assigned to each of the six pFUS exposure parameter sets listed in Table 1 (Low20, High20, Low80, High80, Low1k, High1k). Two sets of animals received sham exposures: one group received the standard Obtx injection, and the other received a saline injection. Starting on d 1, each animal underwent a 15 min-long pFUS treatment or sham exposure once per day as described below, for 4 d. On d 5, the animals were sacrificed, and both left and right tibiae were collected for microCT analysis (described below). The left tibia served as an internal control for the experimental right tibia. The calf muscles were carefully dissected away from the bone and placed in 10% neutral buffered formalin. Samples were cryoprotected before being embedded longitudinally in optimum cutting temperature medium (OCT, Sakura Finetek, Torrance, CA, USA) by immersion in isopentane cooled on dry ice. Eight micrometer sections were stained with hemotoxylin and eosin (H&E) and visualized on an upright microscope (Eclipse 80i, Nikon, Japan).

Pulsed focused ultrasound exposures

Figure 1 depicts a schematic of the experimental setup. Under isoflurane anesthesia and before the ultrasound treatment, hair was thoroughly removed from the right hindlimb of the mouse using depilation lotion (Nair), and the skin was wiped with alcohol to remove cavitation nuclei. Each mouse was placed in a custom holder that extended the right leg such that the pFUS focus could be aligned through the sagittal plane of the calf (lateral to medial) without approaching the bone. The animal holder was attached to a computer-controlled three dimensional (3D) positioning stage (Velmex, Bloomfield NY, USA) to align the calf

midbelly with the transducer focus. With the mouse's head above water, all of the pFUS exposures were performed in a tank of heated (36°C), filtered and degassed water using an air-backed, spherically focused piezoelectric transducer operating at the frequency of 2.158 MHz (45 mm radius of curvature and focal length) that was custom built in-house. The transducer was driven by a function generator (Agilent 33250A, Agilent, Palo Alto, CA, USA) and a power amplifier (150 W, ENI-150, ENI, Rochester, NY, USA). The transducer focus was positioned so that both the focal area (12.6 × 1.9 mm) and the first side lobe would be located within the calf muscle midbelly, without extending to the tibia. This was possible because of the choice of somewhat higher frequency (2 MHz) compared with standard LIPUS frequencies of 1– 1.5 MHz. The calf muscle measured at least 8 mm axially and 6 mm laterally; the focal ultrasound pressure distributions relative to the bone and skin surfaces are illustrated in Figure 2c and d. The lateral alignment was performed by marking the treatment spot on the skin of the calf midbelly and aligning the spot such that it almost touched a removable pointer tip that corresponded to the transducer focus. The pointer was then removed, and the limb was moved 3 mm toward the transducer to adjust the depth of the focus within the calf. This procedure was compared with the focus placement guided by B-mode ultrasound imaging (HDI-1000 scanner with CL10-5 probe, Philips Medical Systems, Bothell, WA, USA) during the first several treatments, and was found to have the same precision.

Six sets of ultrasound exposure parameters were used in this study, as summarized in Table 1. Our choice of the pFUS exposure parameters—ultrasound intensity, pulse duration, pulse repetition frequency and treatment duration—was guided with consideration toward reducing the possibility of damage to the skin or muscle tissue and reducing potential physical effects of ultrasound on the tissues present in the pFUS focus (muscle, fascia, nerve, neuromuscular junction). Based on the literature, the periodic directional tissue displacement caused by acoustic radiation force was hypothesized to be one possible mechanism for tissue stimulation (Gavrilov et al. 1996). The frequency of that displacement, that is, ultrasound pulse repetition frequency (PRF), was chosen to mimic the frequency of motor nerve firing related to either tonic muscle contractions (20 Hz) or walking (80 Hz) (Hennig and Lomo 1985). The third PRF setting of 1 kHz was chosen equal to that used previously by others in LIPUS fracture healing treatments (Azuma et al. 2001; Leung et al. 2004b). The maximum tissue displacement in the direction of ultrasound propagation, occurring at the transducer focus, was estimated using a simplified analytical solution to the inhomogeneous wave equation for elastic solid material (Andreev et al. 1997):

$$\frac{\Delta x = \alpha r_0 I_{\mathrm{SPPA}} t_0}{\rho c_1 c_t} \quad (1)$$

where $\alpha = 0.11$ Np/cm is the coefficient of ultrasound absorption in skeletal muscle; $r = 0.54$ mm is the characteristic transverse ultrasound beam radius, given that the beam profile is approximated by the function $(1 + (r/r_0)^2)^{-3/2}$;I_{SPPA} is the spatial peak pulse average intensity of the ultrasound beam; t_0 is the pulse duration; $\rho = 1041$ kg/m is tissue density; and $c_1 = 1500$ m/s and $c_t = 4$ m/s are the speeds of longitudinal and shear ultrasound wave propagation in tissue, respectively (Duck 1990; Gennisson et al. 2003). At the Low setting,

the tissue displacement was estimated to be 0.09 μm, whereas at the High setting, the tissue displacement was estimated to be 0.18 μm (see Table 1).

The choice of ultrasound intensity was dictated by two factors: avoiding substantial tissue heating and promoting ultrasound-induced cavitation. Tissue heating resulting from ultrasound absorption is known to decrease the nerve conduction velocity reversibly or, above a certain level of heating, irreversibly (Tsui et al. 2005). Ultrasound-induced cavitation is another form of mechanical impact on tissue that is believed to stimulate tissue regeneration in other applications such as bone nonunion healing and wound healing (Elster et al. 2010; Gollwitzer et al. 2013; Kuo et al. 2009). To induce cavitation activity in tissue, the peak rarefactional pressure has to exceed cavitation threshold, which, although still controversial, is believed to be 6.5 MPa (Hwang et al. 2006). Another factor that is known to promote cavitation activity in tissue is the presence of shock fronts in the ultrasound waveform that develop as a result of non-linear propagation effects at high output intensities (Maxwell et al. 2013).

On consideration of all of the above, two acoustic output power settings were chosen that will be referred to as “Low” and “High.” The focal waveforms corresponding to Low and High settings were measured in water at the transducer focus using a fiberoptic probe hydrophone and are illlustrated in Figure 2a. The pressure waveform at the High setting contains a shock front, and the pressure amplitudes (peak positive pressure is 30 MPa, peak negative pressure is 8 MPa) are similar to these used in shock wave therapy of bone non-unions (Elster et al. 2010). At these pressure levels, one would expect cavitation activity in tissue. At the Low setting, the pressure amplitude is lower, but the waveform is still non-linearly distorted, and the pressure levels are similar to those used in ultrasound treatment of diabetic wounds (Kuo et al. 2009). Cavitation is less likely to occur at this level. In the case of a pulse repetition frequency of 1 kHz, both High and Low output levels were adjusted to maintain time-averaged ultrasound intensity similar to that used in the 20 and 80 Hz High and Low groups. The corresponding focal waveforms are shown in Figure 2b.

Pulse durations were chosen to be 5.3 μs, for all exposures. Temperature elevation in the muscle tissue resulting from absorption of a single ultrasound pulse, at each output level, was estimated without taking into account the harmonic content of the non-linearly distorted waveforms and assuming linear absorption; the difference between the two at the intensities used is known to be insignificant (Khokhlova et al. 2009). Heat diffusion was accounted for using an approximate solution for focused transducers derived previously (Parker 1983). The physical properties of murine muscle tissue needed for the calculations were taken from the literature (Duck 1990). In all cases, the maximum estimated temperature elevation per pulse did not exceed 0.01°C to 0.03°C throughout the exposure.

Another physical effect of focused ultrasound that could potentially influence skin and/or muscle tissue is streaming that develops in water close to the transducer focus and may impinge on the water-tissue interface. Flow velocities induced in water by the same focused ultrasound transducer as used here were directly measured in water previously (Al-Qraini et al. 2013) and were found to depend strongly on the focused ultrasound pulse duration. At the pulse duration of 100 μs and peak intensity of 14,000 W/cm^2 , the maximum observed flow

speed was only 2 cm/s. Therefore, under our experimental conditions, this effect could be neglected.

Cavitation detection

To identify whether any of the chosen pFUS exposures induce measurable cavitation activity in the mouse calf muscle, a separate series of *ex vivo* experiments were performed. A total of six animals were used immediately after euthanasia. The general setup was the same as for the pFUS treatment, with the addition of a focused passive cavitation detector (PCD), aligned confocally with the pFUS transducer, as illustrated in Figure 3a. The PCD was a 5 MHz focused piezo-ceramic transducer (aperture = 12.5 mm, radius of curvature = 63.5 mm), with a bandwidth of 3.3–7 MHz at the −6 dB level (Olympus Panametrics NDT-V309). The signals received by the PCD were amplified by 20 dB (Panametrics PR5072, Waltham, MA, USA) and recorded during each pFUS pulse by a digital oscilloscope (LeCroy Wave-Surfer 42Xs) at the sampling frequency of 200 MHz. All muscle samples were subjected to each exposure in Table 1 for 10 s. The signals received by the PCD were analyzed in the frequency domain for broadband noise emissions and ultraharmonic content. The broadband noise level was calculated as a spectral amplitude integral within the frequency band 4.8–5.8 MHz, located between the second and third harmonics of pFUS.

The results of these measurements indicated no cavitation activity in any of the exposures used. The broadband emission level did not exceed the noise level, and the ultraharmonics were not detected even at the highest focal pressure setting and highest PRF (High80). An example of the corresponding PCD signal spectrum is represented in Figure 3b as a *thick black line*. In an attempt to find the cavitation threshold, the pFUS pulse duration at the High80 setting was then gradually increased, and the first signs of cavitation activity were observed when pulse duration exceeded 23–46 μs, for different muscle samples. An example of a PCD signal in the frequency domain, corresponding to a 46 μs pFUS pulse, is represented in Figure 3b as a *gray line*. The broadband noise level is markedly elevated, and the ultraharmonics are clearly visible. Based on the results described above, it was concluded that cavitation activity that is violent enough to be measurable is unlikely to occur during any of the exposures used in this study. However, because any PCD transducer has a finite sensitivity, more subtle cavitation events may have occurred and evaded detection by this system.

Micro-computed tomography

Using a custom alignment device, we conducted all imaging *ex vivo* in the Seattle Craniofacial Center's Small ANimal Tomographic Analysis (SANTA) Facility with a SkyScan 1076 high resolution microCT scanner (Bruker-microCT, Kontich, Belgium) to obtain an 18 μm isotropic voxel resolution image of the proximal tibia in control and experimental hindlimbs. Parameters for scanning were 55 kV tube voltage, 190 μA tube current, no filter, 360 ms integration time and 0.7° rotation step. During each scanning session, flat field correction was completed. Raw data was reconstructed using NRe-con (Bruker-microCT). Thresholding was completed by visual inspection, matching the binary image to the grayscale image.

The specific region of analysis was a 0.9 mm thick section spanning the proximal tibia metaphysis (specifically, the region from the distal edge of the growth plate to 0.9 mm below) to assess and quantify trabecular bone parameters, as analyzed using CTan (Bruker-microCT). Volume renderings of trabecular bone were created using CTVol (Bruker-microCT). Several trabecular bone parameters were assessed and include trabecular bone volume (BV/TV, %), which indicates the fraction of the volume in the assessed region (total volume [TV]) that is filled with mineralized bone (bone volume [BV]); the value will decrease when bone is degraded. Also, specific bone surface (BS/BV, 1/mm) is computed as bone surface (BS) divided by mineralized bone volume (BV) and is a basic parameter used to characterize the complexity of trabecular structures; this parameter will increase with trabecular bone loss. These parameters are used to assess changes in bone volume or bone turnover, respectively. Trabecular bone thickness (Tb.Th, mm) is reported as the mean value of the trabecular structure thickness within the region of interest, in this case the assessed volume in the proximal tibia metaphysis. Trabecular number (Tb.N, 1/mm) represents the number of traversals across the region of interest. Low values of Tb.Th and Tb.N indicate lower stability of the trabecular bone structure. The trabecular pattern factor (Tb.Pf, 1/mm) is a measure of trabecular structure complexity; a low Tb.Pf signifies better connected trabecular lattices, whereas a higher Tb.Pf represents a more degraded trabecular structure. Thus, loss of bone structure is indicated by decreases in trabecular thickness and number and increases in trabecular pattern factor.

Statistical analysis

Within each mouse, the analyses evaluated an experimental limb in comparison to a control limb; therefore, all of the parameters are expressed as percentage change to the experimental limb. Independent *t*-tests were used to evaluate differences in the tibia trabecular bone parameters between the Obtx sham, Saline sham and pFUS treatment groups. All data are reported as means ± standard errors, with $p \leq 0.05$ considered to indicate statistical significance for all comparisons.

RESULTS

All mice included in the analysis visibly displayed paralysis within 24 h of the Obtx injection (lack of ability to extend toes or flex ankle while suspended). If mice did not display paralysis, they were excluded from the study (n = 2, from High20 and Low1k groups). Experiments were performed on groups of mice over the course of five separate experiment sessions, and one set of mice was excluded from the analysis because of insufficient starting weight (minimum weight to participate in the study was 19.5 g). After pFUS exposure and return to consciousness, as a surrogate of pain assessment, we observed each mouse ambulating freely about the cage with no sign of altered weight bearing compared with its pre-exposure gait.

Figure 4 summarizes the results of microCT analysis of bone loss in the different study groups. As expected, the Obtx group exhibited trabecular bone degradation, appearing as a substantial BV/TV loss, increase in BS/ BV, considerable Tb.Th and Tb. N loss and a rise in Tb.Pf. According to the experimental data, bone loss occurred in all groups of mice, but the

loss was diminished by the Low20 pFUS treatment. Because of the method of analysis, *ex vivo* microCT scanning and quantitative comparison of the experimental bone with the contralateral, our results have a standard deviation that is larger than that observed in our previous studies (Poliachik et al. 2010). As such, no statistically significant differences in any of the trabecular bone parameters were observed between the Obtx and Saline sham groups, although the overall trend toward bone degradation was similar to our previous observations. The Saline sham group experienced some bone loss in the injected limb. This may potentially be caused by acute inflammation at the injection site (Stei et al. 1996; Thuilliez et al. 2009), which may have a detrimental effect on bone quality (Elkasrawy et al. 2012).

Overall, the Low20 treatment appears to be most successful at mitigating the changes to trabecular bone architecture in comparison to the Obtx sham group. Although no significant differences were observed in BV/TV between the sham and experimental groups (Fig. 4a), significant mitigation of a rise in BS/BV for the Low20 group was seen compared with the Obtx group, denoting trabecular bone preservation (Fig. 4b). Other parameters describing trabecular bone morphology (Tb.Th, Tb.N and Tb.Pf [Fig. 4c, d, and e, respectively]) also exhibited degradation in all mice, but the Low20 pFUS treatment appeared to diminish these changes, although not statistically significantly.

The other physiologic pFUS exposure using low intensity, Low80, did not influence any of the bone parameters, and the outcome was quite similar to that of the Obtx sham group. In fact, measures of BS/BV and Tb.Pf for the Low80 group were statistically degraded compared with those for the Saline sham group. The treatments that used high ultrasound pressure amplitude and contained shock fronts (High20, High80) did not influence bone loss, with no statistically significant difference from the Obtx sham group, whereas compared with the Saline sham group, the High20 group had statistically significant increases in BS/BV and Tb.Pf. The opposite trend with respect to ultrasound amplitude was observed between the outcomes of the two pFUS treatments mimicking LIPUS (Low1k and High1k). Although the Low1k exposure did not influence bone loss as assessed with all of the reported bone parameters (statistically significant differences between the Low1k and Saline sham groups for Tb.N and Tb.Pf , but not the Obtx group), the High1k exposure led to more moderate degradation in BS/BV and Tb.Pf.

Overall, the data indicate that the Low20 treatment preserved trabecular connections moreso than other treatments and resulted in an outcome very similar to that of the Saline sham group. Examples of trabecular bone volumes from a tibia adjacent to a Low20-treated calf compared with the tibia in the Obtx sham limb and the corresponding contralateral limbs are illustrated in Figure 5.

Figure 6 displays representative images of the histologic sections of the calf muscles stained with H&E. The muscles were collected from mice that were assigned to the following groups: (a) Obtx sham; (b) Low20 treated; (c) High80 treated; (d) Saline sham; (e) a no injection, no treatment control (left calf). None of the analyzed histologic samples displayed evidence of damage that could be attributed to pFUS treatment. Samples in all groups exhibited evidence of localized perifascicular inflammation (e, f). No qualitative differences

were observed between treated and untreated samples. It is worth noting here, however, that the calf muscles were collected 24 h after the last pFUS treatment, and some of the short-lived changes that may have been induced by the subtle cavitation events may not be discernible at that time point. The images provided here, together with the observations from passive cavitation detection, indicate that violent cavitation, such that would result in gross, irreversible changes in muscle fibers, may be ruled out.

DISCUSSION

Our results indicate that pFUS may be a promising tool to mitigate bone loss resulting from paralysis or limited mechanical loading. At least partial mitigation of bone degradation was observed in multiple trabecular bone parameters for one combination of ultrasound exposure parameters—that mimicking the rate of tonic muscle contractions (20 Hz) and non-linearly distorted, without a shock front (Low power). The overall lack of trabecular bone alteration led to significant preservation of specific bone surface (BS/BV) in the Low20 group compared with the Obtx sham group. Interestingly, the Low20 average intensity was the lowest among all the treatment groups (see Table 1) and closely approached the average intensity used by Ferreri et al. (2011) in the LIPUS treatment of osteopenic rat vertebrae (0.1 mW/cm^2). The LIPUS transducer used in that study was flat, with the aperture much larger than rat vertebrae, so that the surrounding muscle was likely affected as well. Whether this was an intended effect or coincidence remains to be determined.

The Low80 treatment, mimicking the rate of muscle contractions during walking, was not as successful at preserving trabecular parameters as the Low20 treatment. The exposures with the focal waveforms containing shock fronts (High20 and High80) at higher output power and higher peak negative pressure were not effective at mitigating bone loss, suggesting that a mild stimulus without shock fronts may be more apt to induce local environmental changes within the muscle that are conducive to positively influencing trabecular bone morphology. The exposures at lower output power with a pulse repetition frequency similar to those used in LIPUS treatment (Low1k and High1k) did not yield a statistically significant benefit with respect to bone loss mitigation.

In considering the physical and biological mechanisms leading to the observed effect, two different interpretations are possible. In the first interpretation, localized acoustic radiation force and the associated tissue displacement are considered a primary physical mechanism. First, acoustic radiation force may influence neural activity by causing localized relative displacement of the peripheral sensory and/or motor nerve membranes and induce excitation of the action potential. Evidence for this mechanism was provided in a number of studies where pFUS at moderate time-averaged intensities stimulated sensory nerve activity (Gavrilov et al. 1996). In turn, bone is highly innervated, and the sympathetic nervous system has been reported to affect bone remodeling (Elefteriou 2005, 2008; Imai and Matsusue 2002; Lam et al. 2012). The tibial nerve supplies sensory innervation to calf muscles and the proximal tibia (Ivanusic 2009), and sensory nerves have been found to influence bone structure (Offley et al. 2005). Thus, the neuronal signaling induced by pFUS in muscle could potentially be muting the signal leading to the osteoclast activation that causes bone loss. As well, acoustic radiation force may affect muscle by causing localized

tissue displacement in the focal area, potentially altering the environment in the adjacent bone through muscle-induced strain. In the second interpretation, acoustic cavitation within the nerve, neuromuscular junction and/or muscle is considered the primary physical mechanism. Although no evidence for cavitation was observed in the PCD measurements performed in this study, the more subtle emissions may have evaded detection. This hypothesis seems more plausible if one considers the possibility for intramembrane cavitation (Krasovitski et al. 2011), which, according to the theory, does not require large pressure amplitudes. If the bubble oscillations in the nerve cause sufficient displacement of the membrane to induce the action potential, neuronal signaling may affect bone remodeling in the similar fashion as in the first interpretation. If the cavitation occurs in the muscle itself, it may induce an array of short-lived molecular responses in the muscle including the upregulation of cytokines, growth factors and adhesion molecules. For example, other authors have observed reversible, transitory opening of the gaps between myofibrils and infiltration by macrophages after the exposure of muscle to pFUS (Burks et al. 2011; Hancock et al. 2009). Some of these molecules stimulate osteoblast proliferation (Chen et al. 2012; Maes and Geert 2008; Marie et al. 2012), though it remains to be seen if release of these factors in muscle can influence bone structure.

In both interpretations, it is not surprising that the Low1k and High1k exposures did not have any effect on bone loss, because the estimated tissue displacement was an order of magnitude smaller than the displacement at other exposure levels, and the peak negative pressure levels were not sufficient to induce intramembrane cavitation. However, the failure and somewhat detrimental effect of exposures performed at the High power setting are better explained by the intramembrane cavitation interpretation. To clarify both the physical cause and the biological pathway, additional studies are needed, in which neuronal signaling, muscle activity and bone mechanical loading would be evaluated during and after pFUS treatment, and osteoblast and osteoclast activity and molecular signaling pathways are evaluated as well. Along with optimizing the specific treatment parameters (daily dose, overall treatment duration), long-term studies are also needed to verify mitigation of bone loss.

As mentioned in the Results section, the study design using the contralateral limb as an internal control led to an increase in the variability in the results. In our previous studies (Poliachik et al. 2010), a serial time point design yielded much more consistent results, in which the affected limb was scanned before the experiment and at specific time points thereafter to assess bone changes within the limb. Therefore, the fact that in the present study one of the metrics of bone loss (BS/BV) reached statistical significance between Obtx- and FUS-treated groups, and other metrics indicated a trend toward statistical significance, suggests that with a better choice of the control, the results may have reached statistical significance. Additionally, we did not assess cortical bone changes in the tibia, because the short duration of the experiment precluded such analyses. In a former study (Poliachik et al. 2010), cortical bone changes were not significant for this dose of Obtx until day 12.

Two previous studies evaluated LIPUS as a means to mitigate postmenopausal or spinal cord injury-induced bone loss in humans (Leung et al. 2004a; Warden et al. 2001b). The LIPUS treatment was not successful in mitigating the bone loss in intact bones. This is likely

due to strong ultrasound reflection at the soft tissue-bone interface, as well as extremely high ultrasound attenuation within human bone cortex that permits ultrasound penetration only into the outermost layers of bone cortex (Warden et al. 2001b). Ultrasound is more successful in treating bone non-unions because the fracture gap allows for ultrasound penetration toward the injured area to induce cavitation and/or microstreaming. It is also worth noting here that bone cortex in small animals that often serve as research models, like rats and rabbits, is much thinner than that in humans, and therefore, ultrasound is more unlikely to penetrate human bone to produce the desired bio-effect.

In considering potential clinical applications of pFUS treatment, it is important to acknowledge that various medical conditions may cause bone loss through different mechanisms, and it is therefore essential to use a relevant animal model of bone loss. The Obtx model used in this study appears to most closely mirror the bone loss resulting from lack of muscle function, such as that resulting from spinal cord injury or stroke. To study microgravity-induced bone loss, many authors have used hindlimb unloading (HU). In a recent study comparing the Obtx model of bone loss to HU, osteoclast recruitment appears to be the dominant mechanism in Obtx-induced bone loss (Aliprantis et al. 2012), whereas bone loss in the HU model appears to be driven by an increase in osteoclast recruitment in conjunction with osteoblast downregulation (Warden et al. 2013). To mimic age-related hormonally induced bone loss in women, ovariectomy has been used, and is characterized as having increased osteoclast and osteoblast activity. The complex environment that occurs with the loss of estrogen leads to general skeletal bone loss (Li et al. 2011). Thus, further studies evaluating pFUS-mitigated bone loss using other animal models are needed to assess its usefulness across bone loss paradigms.

The major potential challenge that may be encountered with this treatment clinically is that the pFUS procedure may cause pain or discomfort to the patient. In fact, it is unlikely that the patient will not feel the treatment at all, because data in the literature indicate that much lower pressure levels and shorter pulses do cause varying sensations, ranging from cold or warm to the sensation of touch and pain (Gavrilov et al. 1977). Elucidating the physical and biological mechanisms of this treatment and defining ultrasound parameter thresholds for bone loss mitigation would help in the search for solutions to alleviate potential pain, such as reducing the pressure level, reducing or increasing the pulse duration or constantly varying the focus location, similar to physical therapy procedures.

CONCLUSIONS

The intent of this study was to evaluate whether pFUS treatment specifically targeting muscle, not bone, could diminish bone loss in mice that were partially paralyzed and did not display typical mechanical loading of the paralyzed limb. We found that pulsed focused ultrasound treatment of paralyzed muscle has the potential to be a promising modality to mitigate paralysis-induced bone loss. In these experiments, we evaluated some of the ultrasound parameters and found that shock waves at high intensities do not appear to be as effective as non-linearly distorted waves at low power. In addition, a PRF of 20 Hz, mimicking the firing rate of postural muscles, appears to be more effective than other PRFs tested here, including the PRF typically used in fracture healing with LIPUS (1 kHz). The

combination of the Low power setting with the PRF of 20 Hz most successfully mitigated bone loss in this model, with 36% of the trabecular bone rescued. Because these experiments targeted muscle alone while specifically avoiding bone, the optimal pFUS parameters identified here may be different from the parameters used in ultrasound treatments applied directly to the bone. Future studies will investigate both mechanical and biological mechanisms of this treatment in an effort to optimize pFUS application.

Acknowledgments

This work was supported, in part, by DoD Award SC090510 and the National Space Biomedical Research Institute through NCC 9-58. The authors thank Ted S. Gross, Department of Orthopaedics, University of Washington, for his generous support of the pilot project that launched this work.

REFERENCES

Al-Qraini MM, Canney MS, Oweis GF. Laser-induced fluorescence thermometry of heating in water from short bursts of high intensity focused ultrasound. Ultrasound Med Biol. 2013; 39:647–659. [PubMed: 23497843]

Aliprantis AO, Stolina M, Kostenuik PJ, Poliachik SL, Warner SE, Bain SD, Gross TS. Transient muscle paralysis degrades bone via rapid osteoclastogenesis. FASEB J. 2012; 26:1110–1118. [PubMed: 22125315]

Andreev VG, Dmitriev VN, Pishchalnikov YA, Rudenko OV. Sapozhnikov OA, Sarvazyan AP Observation of shear waves excited by focused ultrasound in a rubber-like medium. Acoust Phys. 1997; 43:123–128.

Azuma Y, Ito M, Harada Y, Takagi H, Ohta T, Jingushi S. Low-intensity pulsed ultrasound accelerates rat femoral fracture healing by acting on the various cellular reactions in the fracture callus. J Bone Miner Res. 2001; 16:671–680. [PubMed: 11315994]

Belavy DL, Beller G, Armbrecht G, Perschel FH, Fitzner R, Bock O, Borst H, Degner C, Gast U, Felsenberg D. Evidence for an additional effect of whole-body vibration above resistive exercise alone in preventing bone loss during prolonged bed rest. Osteoporos Int. 2011; 22:1581–1591. [PubMed: 20814665]

Body JJ. How to manage postmenopausal osteoporosis? Acta Clin Belg. 2011; 66:443–447. [PubMed: 22338309]

Bolam KA, van Uffelen JG, Taaffe DR. The effect of physical exercise on bone density in middle-aged and older men: A systematic review. Osteoporos Int. 2013; 24:2749–2762. [PubMed: 23552825]

Burks SR, Ziadloo A, Hancock HA, Chaudhry A, Dean DD, Lewis BK, Frenkel V, Frank JA. Investigation of cellular and molecular responses to pulsed focused ultrasound in a mouse model. PLoS One. 2011; 6:e24730. [PubMed: 21931834]

Carvalho DC, Cliquet Junior A. The action of low-intensity pulsed ultrasound in bones of osteopenic rats. Artif Organs. 2004; 28:114–118. [PubMed: 14720297]

Chen HT, Tsou HK, Chang CH, Tang CH. Hepatocyte growth factor increases osteopontin expression in human osteoblasts through PI3K, Akt, c-Src, and AP-1 signaling pathway. PLoS One. 2012; 7:e38378. [PubMed: 22675553]

Cook SD, Salkeld SL, Patron LP, Ryaby JP, Whitecloud TS. Low-intensity pulsed ultrasound improves spinal fusion. Spine J. 2001; 1:246–254. [PubMed: 14588328]

Cusano NE, Bilezikian JP. Combination anabolic and antiresorptive therapy for osteoporosis. Endocrinol Metab Clin North Am. 2012; 41:643–654. [PubMed: 22877434]

Delia Rocca GJ. The science of ultrasound therapy for fracture healing. Indian J Orthop. 2009; 43:121–126. [PubMed: 19777126]

Duck, F. Acoustic properties of tissue at ultrasonic frequencies. London/ New York: Academic Press; 1990.

Elefteriou F. Neuronal signaling and the regulation of bone remodeling. Cell Mol Life Sci. 2005; 62:2339–2349. [PubMed: 16132233]

Elefteriou F. Regulation of bone remodeling by the central and peripheral nervous system. Arch Biochem Biophys. 2008; 473:231–236. [PubMed: 18410742]

Elkasrawy M, Immel D, Wen X, Liu X, Liang LF, Hamrick MW. Immu-nolocalization of myostatin (GDF-8) following musculoskeletal injury and the effects of exogenous myostatin on muscle and bone healing. J Histochem Cytochem. 2012; 60:22–30. [PubMed: 22205678]

Elster EA, Stojadinovic A, Forsberg J, Shawen S, Andersen RC, Schaden W. Extracorporeal shock wave therapy for nonunion of the tibia. J Orthop Trauma. 2010; 24:133–141. [PubMed: 20182248]

Ferreri SL, Talish R, Trandafir T, Qin YX. Mitigation of bone loss with ultrasound induced dynamic mechanical signals in an OVX induced rat model of osteopenia. Bone. 2011; 48:1095–1102. [PubMed: 21241838]

Gavrilov LR, Gersuni GV, Ilyinski OB, Tsirulnikov EM, Shchekanov EE. A study of reception with the use of focused ultrasound: IEffects on the skin and deep receptor structures in man. Brain Res. 1977; 135:265–277. [PubMed: 922476]

Gavrilov LR, Tsirulnikov EM, Davies IA. Application of focused ultrasound for the stimulation of neural structures. Ultrasound Med Biol. 1996; 22:179–192. [PubMed: 8735528]

Gennisson JL, Catheline S, Chaffai S, Fink M. Transient elastography in anisotropic medium: Application to the measurement of slow and fast shear wave speeds in muscles. J Acoust Soc Am. 2003; 114:536–541. [PubMed: 12880065]

Gollwitzer H, Gloeck T, Roessner M, Langer R, Horn C, Gerdesmeyer L, Diehl P. Radial extracorporeal shock wave therapy (rESWT) induces new bone formation in vivo: Results of an animal study in rabbits. Ultrasound Med Biol. 2013; 39:126–133. [PubMed: 23122639]

Hancock HA, Smith LH, Cuesta J, Durrani AK, Angstadt M, Palmeri ML, Kimmel E, Frenkel V. Investigations into pulsed high-intensity focused ultrasound-enhanced delivery: Preliminary evidence for a novel mechanism. Ultrasound Med Biol. 2009; 35:1722–1736. [PubMed: 19616368]

Hennig R, Lomo T. Firing patterns of motor units in normal rats. Nature. 1985; 314:164–166. [PubMed: 3974720]

Hwang JH, Tu J, Brayman AA, Matula TJ, Crum LA. Correlation between inertial cavitation dose and endothelial cell damage in vivo. Ultrasound Med Biol. 2006; 32:1611–1619. [PubMed: 17045882]

Imai S, Matsusue Y. Neuronal regulation of bone metabolism and anab-olism: Calcitonin gene-related peptide-, substance P-, and tyrosine hydroxylase-containing nerves and the bone. Microsc Res Tech. 2002; 58:61–69. [PubMed: 12203704]

Ivanusic JJ. Size, neurochemistry, and segmental distribution of sensory neurons innervating the rat tibia. J Comp Neurol. 2009; 517:276–283. [PubMed: 19757492]

Jiang SD, Dai LY, Jiang LS. Osteoporosis after spinal cord injury. Osteo-poros Int. 2006; 17:180–192.

Khokhlova TD, Canney MS, Lee D, Marro KI, Crum LA, Khokhlova VA, Bailey MR. Magnetic resonance imaging of boiling induced by high intensity focused ultrasound. J Acoust Soc Am. 2009; 125:2420–2431. [PubMed: 19354416]

Khosla S, Melton LJ 3rd, Riggs BL. The unitary model for estrogen deficiency and the pathogenesis of osteoporosis: Is a revision needed? J Bone Miner Res. 2011; 26:441–451. [PubMed: 20928874]

Krasovitski B, Frenkel V, Shoham S, Kimmel E. Intramembrane cavitation as a unifying mechanism for ultrasound-induced bioeffects. Proc Natl Acad Sci USA. 2011; 108:3258–3263. [PubMed: 21300891]

Kuo YR, Wang CT, Wang FS, Chiang YC, Wang CJ. Extracorporeal shock-wave therapy enhanced wound healing via increasing topical blood perfusion and tissue regeneration in a rat model of STZ-induced diabetes. Wound Repair Regen. 2009; 17:522–530. [PubMed: 19614917]

Lacey JV Jr, Mink PJ, Lubin JH, Sherman ME, Troisi R, Hartge P, Schatzkin A, Schairer C. Menopausal hormone replacement therapy and risk of ovarian cancer. JAMA. 2002; 288:334–341. [PubMed: 12117398]

Lam WL, Guo X, Leung KS, Kwong KS. The role of the sensory nerve response in ultrasound accelerated fracture repair. J Bone Joint Surg Br. 2012; 94:1433–1438. [PubMed: 23015574]

Leblanc A, Matsumoto T, Jones J, Shapiro J, Lang T, Shackelford L, Smith SM, Evans H, Spector E, Ploutz-Snyder R, Sibonga J, Keyak J, Nakamura T, Kohri K, Ohshima H. Bisphosphonates as a supplement to exercise to protect bone during long-duration spaceflight. Osteoporos Int. 2013; 24:2105–2114. [PubMed: 23334732]

Leung KS, Lee WS, Cheung WH, Qin L. Lack of efficacy of low-intensity pulsed ultrasound on prevention of postmenopausal bone loss evaluated at the distal radius in older Chinese women. Clin Or-thop Relat Res. 2004a; 427:234–240.

Leung KS, Lee WS, Tsui HF, Liu PP, Cheung WH. Complex tibial fracture outcomes following treatment with low-intensity pulsed ultrasound. Ultrasound Med Biol. 2004b; 30:389–395. [PubMed: 15063521]

Li JY, Tawfeek H, Bedi B, Yang X, Adams J, Gao KY, Zayzafoon M, Weitzmann MN, Pacifici R. Ovariectomy disregulates osteoblast and osteoclast formation through the T-cell receptor CD40 ligand. Proc Natl Acad Sci USA. 2011; 108:768–773. [PubMed: 21187391]

Liu PY, Brummel-Smith K, Ilich JZ. Aerobic exercise and whole-body vibration in offsetting bone loss in older adults. J Aging Res. 2011; 2011:379674. [PubMed: 21253515]

Maes, C.; Geert, C. VEGF in development. Austin, TX: Landes Bioscience; 2008. Vascular and nonvascular roles of VEGF in bone development; p. 79-90.

Manske SL, Boyd SK, Zernicke RF. Vertical ground reaction forces diminish in mice after botulinum toxin injection. J Biomech. 2011; 44:637–643. [PubMed: 21186027]

Marie PJ, Miraoui H, Severe N. FGF/FGFR signaling in bone formation: Progress and perspectives. Growth Factors. 2012; 30:117–123. [PubMed: 22292523]

Marjoribanks J, Farquhar C, Roberts H, Lethaby A. Long term hormone therapy for perimenopausal and postmenopausal women. Cochrane Database Syst Rev. 2012; 7:CD004143. [PubMed: 22786488]

Maxwell AD, Cain CA, Hall TL, Fowlkes JB, Xu Z. Probability of cavitation for single ultrasound pulses applied to tissues and tissue-mimicking materials. Ultrasound Med Biol. 2013; 39:449–465. [PubMed: 23380152]

Offley SC, Guo TZ, Wei T, Clark JD, Vogel H, Lindsey DP, Jacobs CR, Yao W, Lane NE, Kingery WS. Capsaicin-sensitive sensory neurons contribute to the maintenance of trabecular bone integrity. J Bone Miner Res. 2005; 20:257–267. [PubMed: 15647820]

Parker KJ. The thermal pulse decay technique for measuring ultrasonic absorption coefficients. J Acoust Soc Am. 1983; 74:1356–1361.

Poliachik SL, Bain SD, Threet D, Huber P, Gross TS. Transient muscle paralysis disrupts bone homeostasis by rapid degradation of bone morphology. Bone. 2010; 46:18–23. [PubMed: 19857614]

Rawool NM, Goldberg BB, Forsberg F, Winder AA, Hume E. Power Doppler assessment of vascular changes during fracture treatment with low-intensity ultrasound. J Ultrasound Med. 2003; 22:145–153. [PubMed: 12562119]

Schneider V, Oganov V, LeBlanc A, Rakmonov A, Taggart L, Bakulin A, Huntoon C, Grigoriev A, Varonin L. Bone and body mass changes during space flight. Acta Astronaut. 1995; 36:463–466. [PubMed: 11540977]

Sievanen H. Immobilization and bone structure in humans. Arch Bio-chem Biophys. 2010; 503:146–152.

Stei P, Kruss B, Wiegleb J, Trach V. Local tissue tolerability of melox-icam, a new NSAID: Indications for parenteral, dermal and mucosal administration. Br J Rheumatol. 1996; 35(Suppl 1): 44–50. [PubMed: 8630637]

Thuilliez C, Dorso L, Howroyd P, Gould S, Chanut F, Burnett R. Histo-pathological lesions following intramuscular administration of saline in laboratory rodents and rabbits. Exp Toxicol Pathol. 2009; 61:13–21. [PubMed: 18835765]

Tsui PH, Wang SH, Huang CC. In vitro effects of ultrasound with different energies on the conduction properties of neural tissue. Ultrasonics. 2005; 43:560–565. [PubMed: 15950031]

van der Jagt OP, Waarsing JH, Kops N, Schaden W, Jahr H, Verhaar JA, Weinans H. Unfocused extracorporeal shock waves induce anabolic effects in osteoporotic rats. J Orthop Res. 2013; 31:768–775. [PubMed: 23239548]

Warden SJ, Bennell KL, Forwood MR, McMeeken JM, Wark JD. Skeletal effects of low-intensity pulsed ultrasound on the ovariectomized rodent. Ultrasound Med Biol. 2001a; 27:989–998. [PubMed: 11476933]

Warden SJ, Bennell KL, Matthews B, Brown DJ, McMeeken JM, Wark JD. Efficacy of low-intensity pulsed ultrasound in the prevention of osteoporosis following spinal cord injury. Bone. 2001b; 29:431–436. [PubMed: 11704494]

Warden SJ, Galley MR, Richard JS, George LA, Dirks RC, Guildenbecher EA, Judd AM, Robling AG, Fuchs RK. Reduced gravitational loading does not account for the skeletal effect of botulinum toxin-induced muscle inhibition suggesting a direct effect of muscle on bone. Bone. 2013; 54:98–105. [PubMed: 23388417]

Warner SE, Sanford DA, Becker BA, Bain SD, Srinivasan S, Gross TS. Botox induced muscle paralysis rapidly degrades bone. Bone. 2006; 38:257–264. [PubMed: 16185943]

Williams D, Kuipers A, Mukai C, Thirsk R. Acclimation during space flight: Effects on human physiology. CMAJ. 2009; 180:1317–1323. [PubMed: 19509005]

Wronski TJ, Lowry PL, Walsh CC, Ignaszewski LA. Skeletal alterations in ovariectomized rats. Calcif Tissue Int. 1985; 37:324–328. [PubMed: 3926284]

Yang RS, Chen YZ, Huang TH, Tang CH, Fu WM, Lu BY, Lin WL. The effects of low-intensity ultrasound on growing bone after sciatic neurectomy. Ultrasound Med Biol. 2005; 31:431–437. [PubMed: 15749567]

Zelle BA, Gollwitzer H, Zlowodzki M, Buhren V. Extracorporeal shock wave therapy: Current evidence. J Orthop Trauma. 2010; 24(Suppl 1):S66–S70. [PubMed: 20182240]

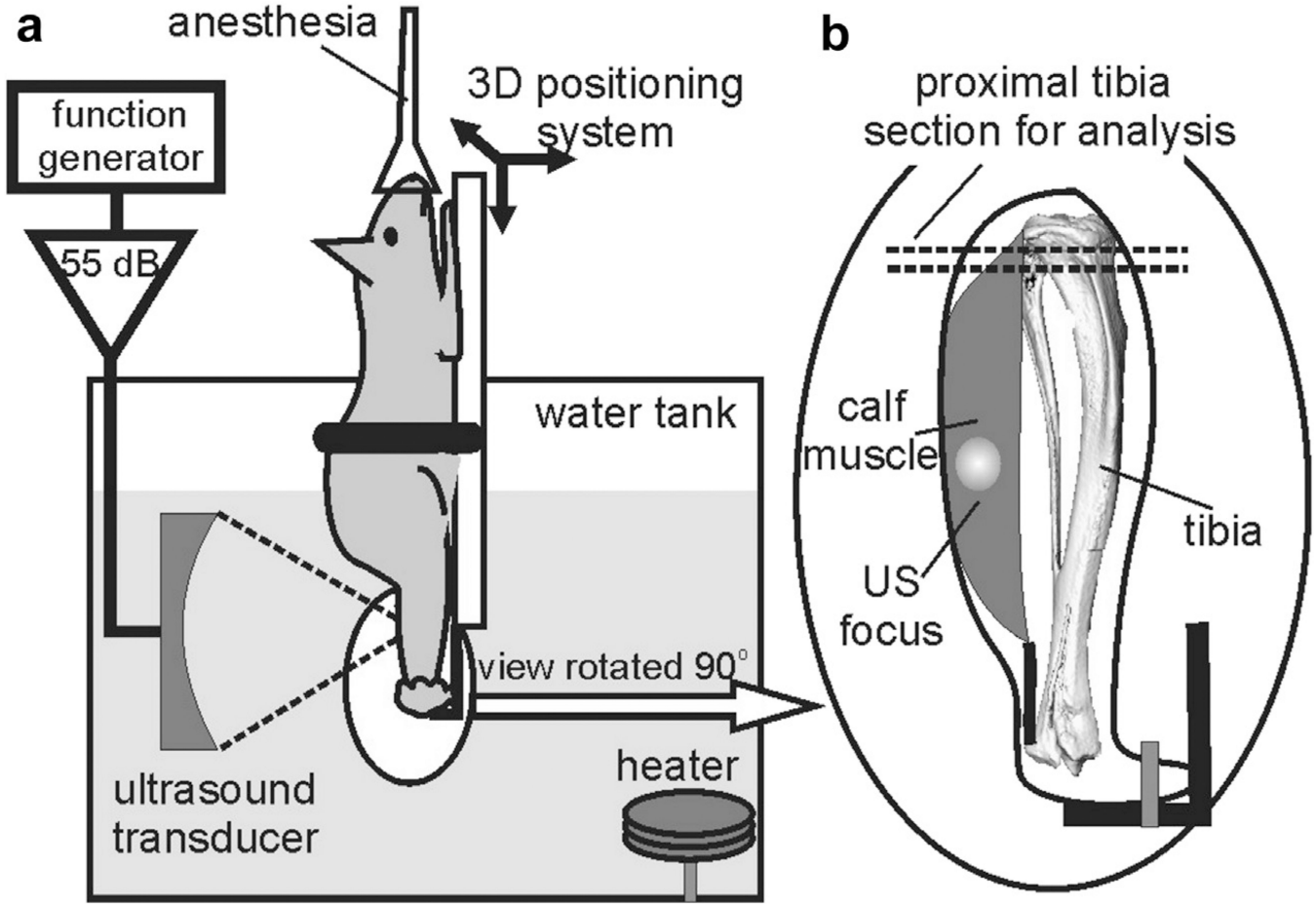

Fig. 1.

(a) Experimental setup for pulsed focused ultrasound (pFUS) treatment of the mouse calf muscle, as described in the text. Treatments were performed in a heated water bath to ensure good acoustic coupling, (b) The leg is rotated 90°, and the positioning of the ultrasound focus is indicated. The long axis of the transducer focus lies completely within the muscle midbelly without approaching the tibia. The region of micro-computed tomography analysis is noted in the proximal tibia.

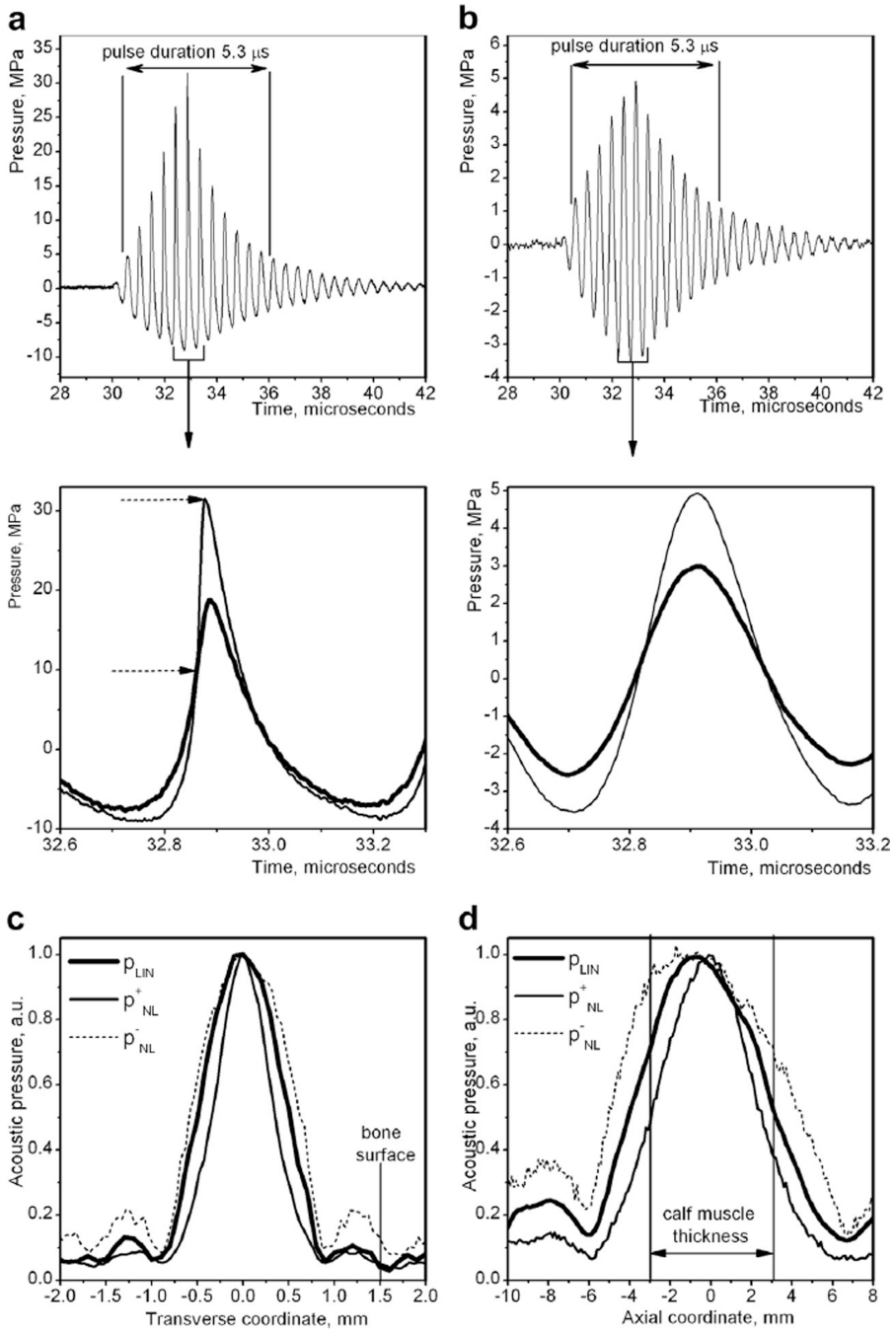

Fig. 2.

Ultrasound fields produced by the 2 MHz transducer, as measured by the fiberoptic probe hydrophone in water. (a) Non-linearly distorted ultrasound pulses, measured at the focus, used in the exposures with 20 and 80 Hz pulse repetition frequencies (top), and detailed view of the highest amplitude section of the pulse produced with “High” (*thin line*) and “Low” (*thick line*) power output settings (bottom). *Dashed arrows* mark the shock front that forms in the case of the “High” setting. (b) Lower amplitude, linear pulses used in the exposures with 1 kHz pulse repetition frequency (top), and detailed view of the highest

amplitude section of the pulse (bottom). (c, d) Peak pressure distributions in the focal region across (c) and along (d) the transducer axis, in linear (*thick line*) and non-linear regimes (*thin line* for peak positive pressure and *dotted line* for peak negative pressure). The *vertical lines* mark the relative position of the tibia (c) and the skin-water boundaries (d). As seen, the focus was placed so that the calf would be affected directly by the main lobe. The second side lobe was incident on the tibia, whereas the first side lobe could potentially affect it in some cases because of small inaccuracies in positioning of the limb (±0.25 mm). However, the side lobes were unlikely to produce any bioeffect inside the bone because of the very short pulse duration and low amplitude. The maximum peak negative pressure at the bone surface (High80 exposure) was 20% of the peak negative pressure in the main lobe, or 1.8 MPa (corresponding mechanical index = 1.2), and the maximum peak positive pressure was 2.1 MPa.

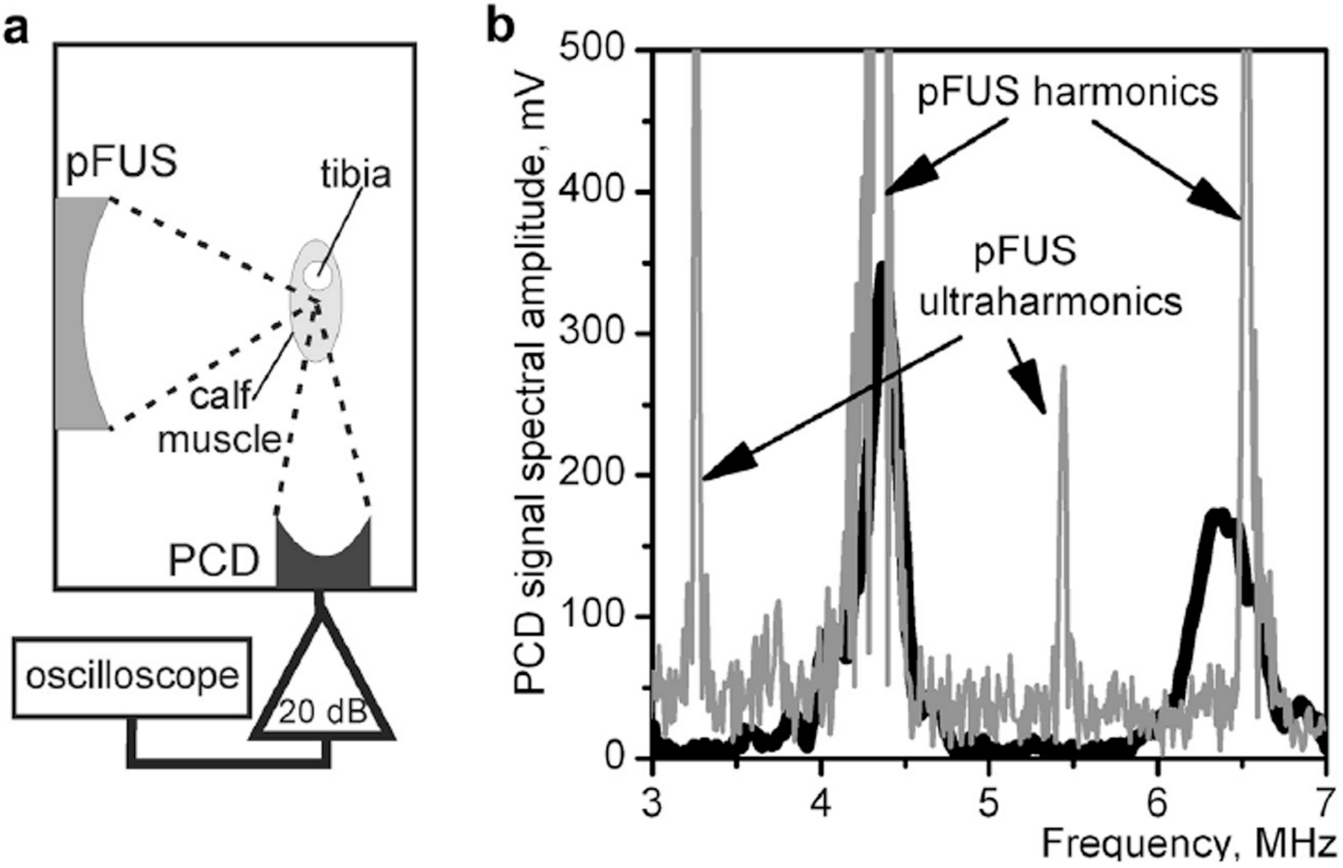

Fig. 3.

Passive cavitation detection (PCD) in *ex vivo* murine calf muscles (n = 6) was performed during each pulsed focus ultrasound (pFUS) exposure listed in Table 1. (a) Measurement arrangement: The 5 MHz PCD transducer was positioned confocally with the pFUS transducer. (b) Cavitation occurrence, as measured by the level of broadband noise emissions and the amplitude of ultraharmonics, was not observed in any of the pFUS exposures, even at the highest focal pressure level (High80). To induce measurable cavitation activity, the pulse duration had to be increased from 5.3 μs up to 23–46 μs at the High80 setting. Examples are provided of the spectral amplitude of PCD signals recorded during a 53-μs pulse (*black line*) and a 46-μs pulse (*gray line*), in which the presence of broadband noise and ultraharmonics is clear.

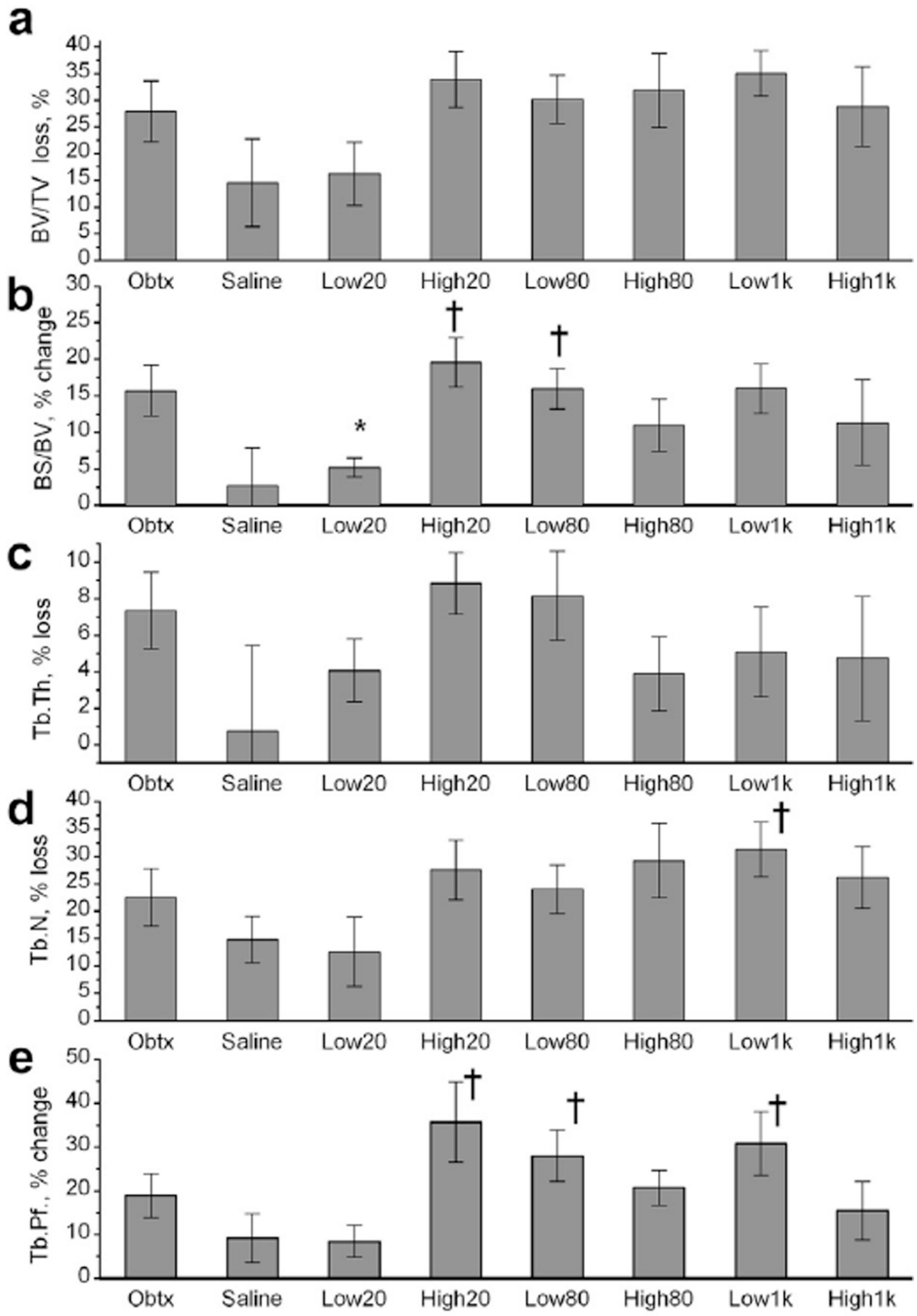

Fig. 4.

Trabecular bone loss in mouse proximal tibia 5 d after onabotulinumtoxinA (Obtx)-induced paralysis of the calf muscle and pulsed focused ultrasound (pFUS) treatment of the muscle, evaluated with *ex vivo* micro-computed tomography. The results are expressed as percentage change relative to the contralateral, non-experimental limb. (a) BV/TV (bone volume/total volume) = Trabecular bone volume: higher loss indicates bone degradation. (b) BS/BV = specific bone surface: higher change indicates bone loss. (c) Tb.Th = trabecular thickness: higher loss indicates bone degradation; (d) Tb.N = trabecular number: higher loss indicates

bone degradation. (e) Tb.Pf = trabecular pattern factor: higher change indicates bone loss. Treatment group abbreviations are described in Table 1. Animals per group: Obtx sham, n = 7; Saline sham, n = 6; Low20, n = 6, High20, n = 6; Low80, n = 7; High80, n = 5; Low1k, n = 5; High1k, n = 6. Data are presented as averages ± standard errors. *Significant difference from the Obtx sham group at $p < 0.05$. †Significant difference from the Saline sham group at $p < 0.05$.

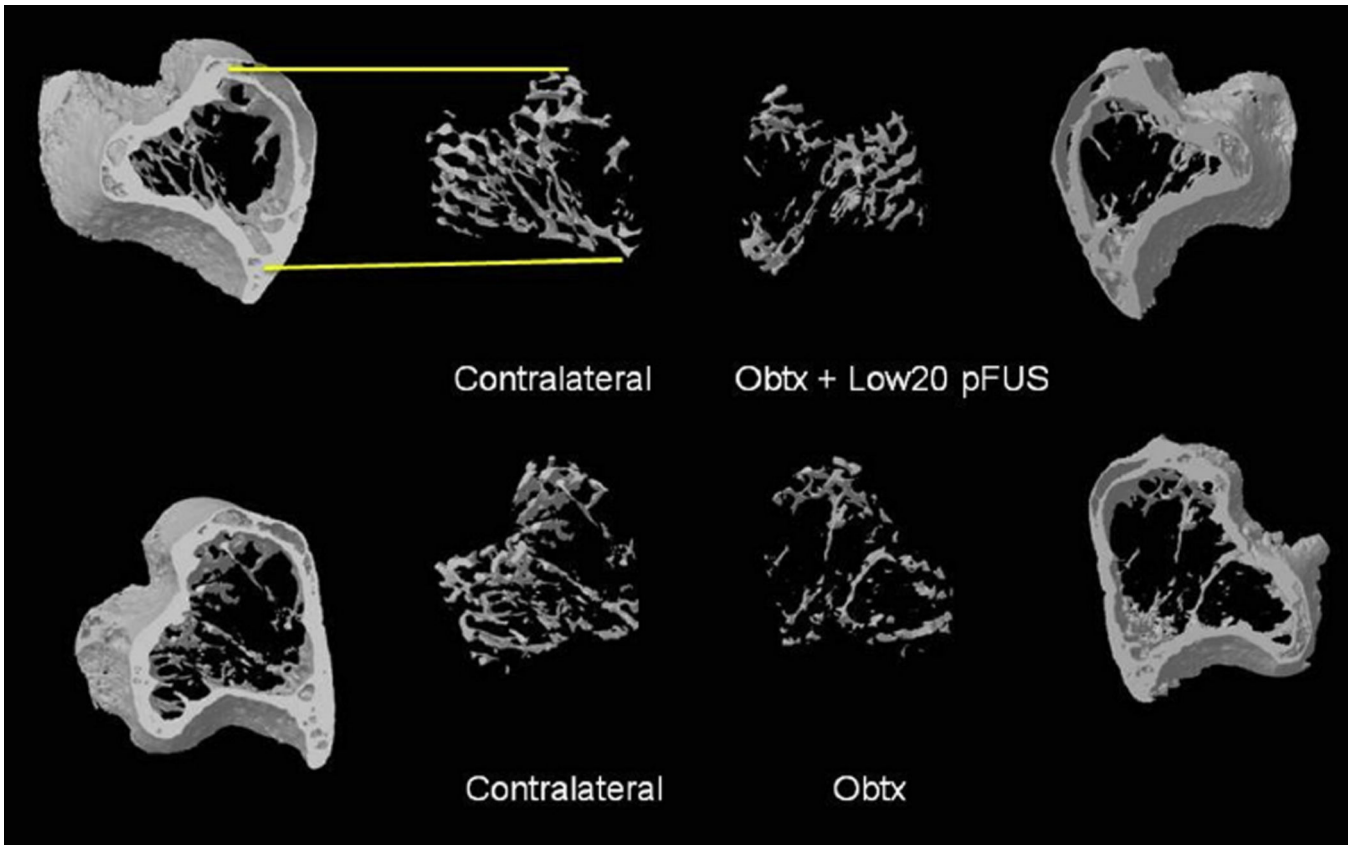

Fig. 5.

Example images of 3D volume renderings of micro-computed tomography data reveal the proximal tibia with the trabecular bone extracted in both the experimental (*right*) and contralateral (*left*) limbs. Top: Animal injected with ona-botulinumtoxinA (Obtx) and treated with pulsed focused ultrasound (pFUS) using the Low20 treatment protocol. Bottom: Animal from the Obtx sham group. This image qualitatively indicates the ability of pFUS treatment of the paralyzed muscle to mitigate paralysis-induced trabecular bone loss (Obtx + Low20 pFUS). Mean values for the different parameters characterizing bone loss for all experimental and sham groups are given in Figure 4.

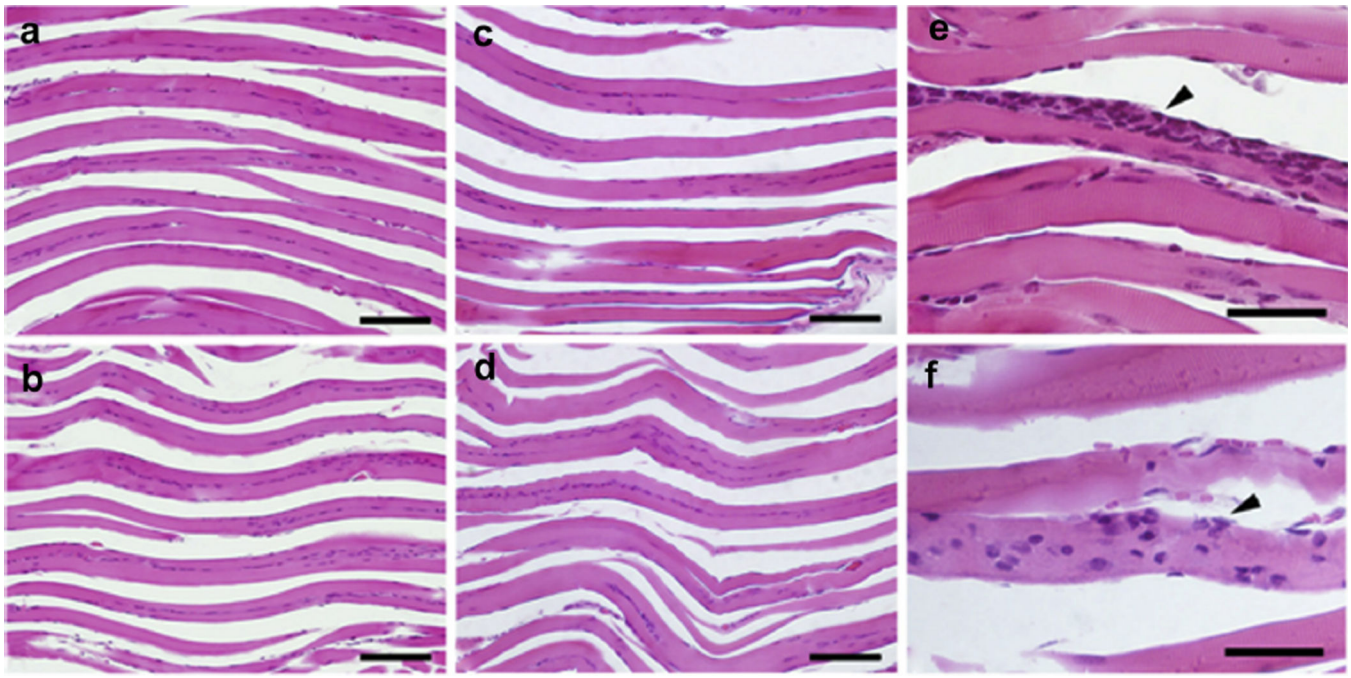

Fig. 6.

Representative histologic images of formalin-fixed calf muscle stained with H&E. Images reveal longitudinal muscle fibers (pink) with nuclei (purple). No damage was detected in the (a) Obtx sham, (b) Low20-treated, (c) High80-treated, or Saline sham (image not shown) limb compared with (d) an uninjected contralateral limb. There was some evidence of localized mild perifascicular inflammation in many of the injected tissue muscles, whether sham treated or ultrasound treated. Examples of inflammation *{arrowhead*) in Obtx sham (e) and High80-treated (f) samples are presented. Bar = 100 μm (a–d) and 40 μm (e–f).

Table 1

Pulsed focused ultrasound exposure parameters for different treatment groups

Treatment type	p^+ (MPa)	p^- (MPa)	PRF (Hz)	I_{SPPA} (W/cm^2)	I_{SPTA}(W/cm^2)	ΔT(°C)	Δx (μm)
Low20	19	7	20	1886	0.2	0.0005	0.09
High20	31	9	20	3554	0.38	0.001	0.18
Low80	19	7	80	1886	0.8	0.0005	0.09
High80	31	9	80	3554	1.5	0.001	0.18
Low1k*	3	2.6	1000	125	0.8	4*e*-5	0.006
High1k*	5	3.5	1000	283	1.5	9*e*-5	0.014

$p+$ and p^- = peak positive and peak negative pressures in the waveform, respectively; PRF = pulse repetition frequency; I_{SPPA} = spatial peak, pulse average intensity; I_{SPTA} = spatial peak, time averaged intensity; ΔT = estimated maximum temperature elevation in muscle resulting from a single ultrasound pulse; Δx = estimated muscle tissue displacement resulting from radiation force exerted by a single ultrasound pulse.

* The Low1k and Highlk exposures were designed to mimic the PRF used in low-intensity pulsed ultrasound (LIPUS) treatments (1 kHz), and have the same I_{SPTA} values as Low80 and High80 exposures. In comparison, the LIPUS treatments typically operate at I_{SATA} of 5–100 mW/cm^2 and 20% duty factor. LIPUS intensity of 100 mW/cm^2 was found to be the minimum intensity that mitigated bone loss in osteopenic animals (Ferreri et al. 2011).